ELSEVIER

Fluid Phase Equilibria 166 (1999) 21–37

FLUID PHASE EQUILIBRIA

www.elsevier.nl/locate/fluid

A novel approach to thermophysical properties prediction for chloro-fluoro-hydrocarbons

Maurizio Fermeglia *, Sabrina Pricl

Department of Chemical, Environmental and Raw Materials Engineering-DICAMP, University of Trieste, Piazzale Europa 1, I-34127 Trieste, Italy

Received 11 January 1999; accepted 8 September 1999

Abstract

In this paper we present a new procedure, based on quantum/molecular (QM/MM) mechanics and molecular dynamics (MD) computer simulations, for estimating the Perturbed Hard Sphere Chain Theory (PHSCT) equation of state (EOS) parameters of a set of 14 alternative chloro-fluoro-hydrocarbons (CFH) of industrial relevance and to predict their thermophysical properties and PVT behavior. Force field and quantum-mechanical techniques were employed in molecular modeling and for the calculation of geometrical and chemico-physical parameters. The Connolly surface algorithm, corrected for quantum-mechanical effects, was used in the evaluation of molecular surfaces and volumes. From these data, the parameters of the PHSCT EOS, V^* and A^*, were obtained. The third parameter, E^*, was calculated from extensive MD simulations under NPT conditions. The new, original method proposed in this work gives good results, is relatively inexpensive, is absolutely general and can be applied in principle to any EOS, provided the parameters have a physical meaning. The tuning of the energetic parameter to a generated data set accounts for the degree of empiricism introduced at a certain stage in the development of any EOS.

Keywords: Equation of state; Refrigerants; Vapor–liquid equilibria; Thermophysical properties; Molecular simulation; Molecular dynamics

1. Introduction

The year 2000 will ratify the definitive banning of ozone damaging substances such as fully chlorinated hydrocarbons used as working fluids in existing refrigeration units. This undoubtedly will give rise to a great deal of research activity in the field, looking for new alternatives. It is well known

* Corresponding author. Tel.: +0039-40-6763438; fax: +0039-40-569823; e-mail: mauf@dicamp.univ.trieste.it

0378-3812/99/$ - see front matter
PII: S0378-3812(99)00295-2

that no existing pure fluids can ensure performances equal or at least comparable to those of the substances to be banned; therefore, the main interest will be devoted to mixtures. Azeotropic mixtures, used so far as alternatives to pure components, do not possess the required flexibility to exhibit thermophysical properties at least close to those of the substances to be banned. For this reason, zeotropic mixtures are now considered as alternative refrigerant fluids but, for these mixtures, the availability of a predictive tool for the calculation of phase equilibria is of paramount importance in the selection of the correct process fluids. However, the number of potentially useful mixtures is huge, and it would be extremely uneconomical, if not even inconceivable, to evaluate experimentally the thermodynamic properties of all possible alternatives.

Nevertheless, it might be not so for a computer. In fact, computer experiments provide a direct route from the microscopic details of a system (masses and charges of atoms, interatomic forces, molecular geometries, etc.) to macroscopic characteristics of experimental interest, such as equations of state, transport properties, and so on. As well as being of academic interest, virtual experiments can become technologically useful. Let us consider again the possible candidate mixtures for alternative refrigerants. The cost of collecting one vapor–liquid equilibria (VLE) data point (i.e., one temperature and composition for just one binary mixture) has been estimated to be around US$2600 and to take 2 days [1]. Thus, we can reasonably hope to perform an experimental characterization of VLE for a minute fraction of the total possible mixtures, temperatures and compositions. With the computing power and technology available nowadays, computer molecular simulations can be considered cheaper and faster than true experiments, especially for simple molecular fluids. Therefore, provided we properly account for the two major problems encountered in any virtual experiment (i.e., the size of the configurational space that is accessible to the molecular system and the accuracy of the molecular model or atomic interaction function or force field that is used to model the molecular system), we can think of computer simulation at least as a first way of screening among the plethora of possible system candidates.

Indeed, during the last decades virtual experiments based on quantum/molecular (QM/MM) mechanics calculations and molecular dynamics (MD) simulation techniques have opened avenues in the estimation and prevision of thermophysical properties (both under equilibrium and non-equilibrium conditions) of simple molecular fluids. The treatment of molecular systems in the vapor/gas phase by quantum mechanics is quite simple, due to the possibility of reducing the many-particle problem to a few-particle one based on the low density of a system in the gas phase. If the classical statistical mechanics approximation is permitted, the problem becomes even simpler. Nevertheless, for both amorphous solid states and liquid systems such as solutions and polymers we remain faced with an essentially many-particle systems, for which no simple reduction to a few degrees of freedom is possible, and a full treatment of many degrees of freedom is necessary to adequately describe the properties of molecular systems in the fluid-like state. In such cases, to obtain reliable estimations of dynamic and non-equilibrium properties dynamic simulation methods that produce trajectories in the phase space are to be used. The method of MD solves Newton's equation of motion for a given molecular system, which results in space trajectories for all atoms in the system. From these atomic trajectories, a plethora of thermophysical properties can then be calculated as time averages from the relevant microscopic relationships expressed in terms of molecular positions and momenta.

As mentioned above, the aim of computer simulations of molecular systems is to compute macroscopic behavior from microscopic interactions. The major contributions a microscopic consideration can afford are (a) the understanding and (b) interpretation of experimental results, (c)

semiquantitative estimates of experimental results, and last but not least, (d) the possibility to interpolate or extrapolate experimental data into regions that are only difficultly realizable, if at all, in the laboratory.

The specific problem of the computer simulation of alternative refrigerants has been initially approached via MD in different conditions by Bohm et al. [2] using a potential derived from ab initio calculations and fitted to second virial coefficients, by Gough et al. [3] using the well-known AMBER potential function [4] and by Vega et al. [5]. Yamamoto et al. [6] performed MonteCarlo simulations for several fluoropropane type alternative refrigerants. Lisal and Vacek [7,8] obtained excellent results for ethane-type alternative liquid refrigerants by using a new potential that can absorb multibody interactions and other contributions in a mean field. All the above-cited authors have concentrated their efforts in the development of new force field potentials. In this paper we want to show how, from such experiments it is possible to extract the characteristic parameters of some equation of state (EOS), thus avoiding tedious experimental effort for determining PVT isotherms and vapor pressure as a function of temperature. To this aim we report our recent progress in the attempt of combining the technique of MM/MD and the EOS theory. Basically, we developed a strategy for calculating the parameters A^*, V^* and E^* characteristic of the Perturbed Hard Sphere Chain Theory (PHSCT) EOS as reformulated by Fermeglia et al. [9,10] for a series of possible alternative refrigerants. According to our procedure, the first two EOS parameters A^* and V^* can be obtained from a combination of MM and graphical algorithms, whereas the third, energetic parameter E^* can be obtained from MD simulations in the gas state. With the EOS parameter values calculated according to this maneuver, we predicted the VLE and PVT behavior of the considered systems in a vast range of T and P values and compared the results of this prediction with the available experimental data. As we shall discuss later in more detail, the quality of the prediction, in conjunction with the relatively fast calculation time required for the simulation, can be considered extremely satisfactory. Furthermore, although a specific EOS has been considered here, the proposed computational procedure holds an absolutely general character and can be applied to any EOS, on condition that its characteristic parameters have a sound and well defined physical meaning [11].

In our opinion, this procedure could be of great help in integrating MD techniques and process simulators, particularly in those cases where EOS parameters must be obtained for molecules with scarce if not absent experimental data sets available.

2. Computer simulation methodology

All simulations were run on a Silicon Graphics Origin 200 and performed by using the commercial software Cerius^2 (v. 3.5) from Molecular Simulation (for both MM/QM and MD simulations) and in-house developed computer programs (stand-alone and add-on to the commercial package). The generation of accurate model structures of 14 chloro-fluoro-hydrocarbon (CFH) molecules was conducted as follows. For each CFH, the molecule was built and its geometry optimized via energy minimization using the COMPASS 1.0 force field. The COMPASS FF is an augmented version of the CFF series of force fields [12–15] and is the first ab initio force field that has been parameterized and validated using condensed-phase properties in addition to various ab initio and empirical data for molecules in isolation. The bond terms of the COMPASS FF potential energy function include a

quartic polynomial both for bond stretching and angle bending, a three-term Fourier expansion for torsions and a Wilson out-of-plane coordinate term. Six crossterms up through the 3rd order are present to account for coupling between the intramolecular coordinates. The final two nonbonded terms represent the intermolecular electrostatic energy and the van der Waals interactions, respectively; the latter employs an inverse 9th power term for the repulsive part rather than the more customary 12th power term (see Appendix A for details).

The molecules were modeled to have a total charge equal to zero, and the distribution of the partial charge within each molecule was determined by the charge equilibration method of Rappé and Goddard [16]. Energy was minimized by up to 5000 Newton–Raphson iterations. Following this procedure, the root-mean-square (rms) atomic derivatives in the low energy regions were smaller than 0.05 kcal/mole Å. Long-range nonbonded interactions were treated by applying suitable cut-off distances, and to avoid the discontinuities caused by direct cutoffs, the cubic spline switching method was used [17]. van der Waals distances and energy parameters for nonbonded interactions between heteronuclear atoms were obtained by the 6th-power combination rule proposed by Waldman and Hagler [18]. Other chemico-physical parameters were obtained by the semi-empirical quantum-mechanical algorithm MOPAC (v. 6.0), using the AM1 method and the BFGS procedure with the PRECISE option selected to ensure an adequate convergence criterion. Following this protocol, the maximum residual internal coordinate forces on the optimized coordinates were always less than 3×10^{-4} hartree/bohr. The stopping criterion for the SCF iterative process required a density matrix convergence of less than 10^{-8}.

The calculations of molecular surfaces were performed using the so-called Connolly dot surfaces algorithm [19–21]. Accordingly, a probe sphere of a given radius, representing the solvent molecule, is placed tangent to the atoms of the molecule at thousands of different positions. For each position in which the probe does not experience van der Waals overlap with the atoms of the molecule, points lying on the inward-facing surface of the probe sphere become part of the molecule solvent-accessible surface. According to this procedure, the molecular surface generated consists of the van der Waals surface of the atoms which can be touched by a solvent-sized probe sphere (thus called contact surface), connected by a network of concave and saddle surfaces (globally called reentrant surface), that smooths over crevices and pits between the atoms of the molecule. The sum of the contact and the reentrant surface form the so-called molecular surface (MS); this surface is the boundary of the molecular volume (MV) that the solvent probe is excluded from if it is not to undergo overlaps with the molecule atoms, which therefore is also called solvent-excluded volume. Finally, performing the same procedure by setting the probe sphere radius equal to zero, the algorithm yields the van der Waals surface (WS).

If the Connolly algorithm can be considered a good technique for calculating molecular surfaces, the same procedure has been proved to be less accurate for the determination of molecular volumes. Indeed, it has been observed that the molecular volumes derived using algorithms based on van der Waals radii are generally 30% lower than the experimentally determined volumes for small molecules [22]. Accordingly, for the calculation of the CFHs molecular volumes, we employed a method based on semiempirical molecular orbital calculations. First, the electron density distribution of the molecule was determined using the AM1 algorithm. The software calculates the electron density of the molecule at each point of a grid covering the molecule, allowing the grid size and the space between grid points to be varied. Since the orientation of the molecule within the grid can also be varied, the errors that occur from using a grid of a specific spacing and size can be quantified. The electron

density value for each point of the grid was then used to calculate the volume of each molecule as a function of the percentage of the total, calculated electronic density, according to a calculation technique proposed by Rellick and Becktel [22]. In this way, no assumption was made about the value of the radii of individual atoms or groups of atoms. Fig. 1(a) and (b) report two examples of Connolly surfaces obtained for the refrigerants R22 and R142b, respectively.

For the calculation of the thermophysical properties of CFHs, 256 molecules were confined in a cubic box with periodic boundary conditions; in order to minimize the artifact of periodicity for liquids and gases, a cut-off distance was set equal to half the box length. The resultant structures were relaxed via MM, again using the COMPASS FF; in this case, the Ewald technique was employed in handling nonbonded interactions.

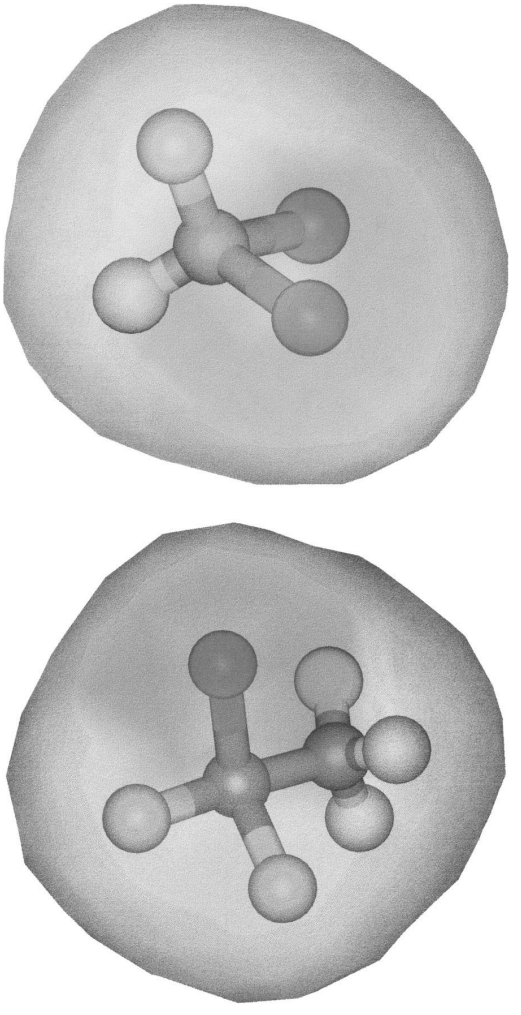

Fig. 1. (a) Connolly surfaces calculated for the refrigerant R22. (b) Connolly surface calculated for the refrigerant R142b.

Each constant pressure–constant temperature (NPT) MD run was started by assigning initial velocity for the atoms according to a Boltzmann distribution at $2 \times T$. Temperature was controlled via weak coupling to a temperature bath [23], with coupling constant $\tau_T = 0.01$ ps, whereas pressure was kept constant by coupling to a pressure bath [24], with relaxation time $\tau_P = 0.1$ ps. The Newton molecular equations of motion were solved by the Verlet leapfrog algorithm [25], using an integration step of 1 fs. Since the partial charges assigned by the charge equilibration method are dependent on structure geometry, they were updated regularly every 100 MD steps during the entire MD runs.

Each MD simulation was performed using the COMPASS force field and consisted in a system equilibration phase, during which the equilibration process was followed by monitoring the behavior of both kinetic and potential energy and the time evolution of density, and a successive data collection phase. For the CFHs liquid state simulation, the energy components as well as density have ceased to show a systematic drift and have started to oscillate about steady mean values around 30 ps. Even shorter times were required to equilibrate the vapor/gas phase. Accordingly, equilibration phases longer than 50 ps (i.e., 50,000 MD steps with time step = 1 fs) and data acquisition runs longer than 250 ps were judged not necessary to enhance data accuracy. An example of the behavior of the total, kinetic and potential energy vs. time and the time evolution of density (during the equilibration phase only) for R113 at 600 K is given in Fig. 2(a) and (b), respectively.

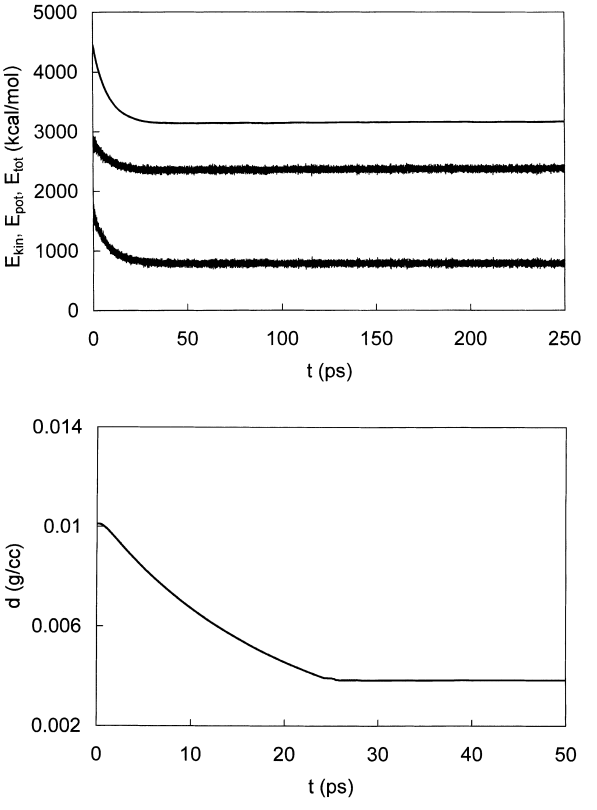

Fig. 2. (a) Time behavior of the energy components during 250 ps of NPT simulation of R113 at 600 K. Top curve: total energy (E_{tot}); middle curve: kinetic energy (E_{kin}); bottom curve: potential energy (E_{pot}). (b) Time evolution of density during the first 50 ps (equilibration phase) of NPT simulation of R113 at 600 K.

3. Theory

The EOS considered in this work is based on the simplified PHSCT model [26–29], in which the molecule is considered being constituted by chains of freely jointed tangent hard spheres (or segments). The PHSCT EOS has been developed starting from the modified Chiew EOS for hard-sphere chains as the reference term [30], a van der Waals-type perturbation term and the Song–Mason method [26] to relate EOS parameters to the intermolecular potential.

In term of pressure, the complete EOS can be expressed as:

$$\frac{P}{\rho kT} = 1 + r^2 b\rho g(d^+) - (r-1)\left[g(d^+) - 1\right] - \frac{r^2 a\rho}{kT} \tag{1}$$

where P is the pressure, T the absolute temperature, $\rho = N/V$ the number density, N the number of molecules, V the volume of the system, k the Boltzmann constant, d the hard-sphere diameter and $g(d^+)$ the pair radial distribution function of hard spheres at contact. Eq. (1) contains three parameters, all with a well-defined physical meaning: the number of effective hard spheres per molecule (r), the intermolecular potential-well depth between a nonbonded pair of segments (a) and the effective hard-sphere diameter (b).

To obtain an engineering-oriented EOS, a redefinition of the EOS parameters has been performed [9,10,26] as follows. The attractive parameter a and the effective hard-sphere diameter b were recast in terms of constants associated with intermolecular potentials and represented by two functions of temperatures:

$$a(T) = \frac{2\pi}{3}\sigma^3\varepsilon F_a(kT/\varepsilon) \tag{2}$$

$$b(T) = \frac{2\pi}{3}\sigma^3\varepsilon F_b(kT/\varepsilon) \tag{3}$$

where ε and σ are the pair potential parameters: ε is the depth of the minimum in the pair potential and σ is the separation distance between segment centers at this minimum. F_a and F_b are two universal functions given by empirical equations determined from thermodynamic properties of argon and methane over a large range of temperature and density [29].

In summary, each pure component was characterized by a set of three segment-based parameters — σ, ε and r — which were combined further to yield three, final characteristic molecular parameters reflecting the size, shape and energetic interactions of the fluids considered as follows. First, a characteristic volume V^* was defined as:

$$V^* = (\pi/6) r\sigma^3 N_A \tag{4}$$

where N_A is Avogadro's constant. Second, a characteristic surface area, A^*, was given as:

$$A^* = \pi r\sigma^2 N_A \tag{5}$$

and finally a characteristic ''cohesive'' energy, E^* was introduced as:

$$E^* = r(\varepsilon/k) R_g \tag{6}$$

Table 1
Structural molecular parameters and selected chemico-physical data for all CFHs
Comparison between calculated and experimental data (in parenthesis, where available).
ΔH_{form} = enthalpy of formation; I.P. = ionization potential; μ = dipole moment.

CFHs	Bond lengths (Å), bond angles (°)	ΔH_{form} (kcal/mol)	I.P. (eV)	μ (D)
R13				
C–F	1.320 (1.325)			
C–Cl	1.750 (1.752)	−162.6 (−168.8)	13.2 (12.4)	0.59 (0.50)
FCF	108.3 (108.6)			
R14				
C–F	1.322 (1.323)	−225.7 (−223.1)	15.3	0
FCF	109.4 (109.5)			
R21				
C–F	1.338			
C–Cl	1.767			
C–H	1.101			
FCCl	110.2	−65.22	12.0 (11.5)	1.39 (1.29)
ClCCl	110.7			
FCH	109.4			
ClCH	108.2			
R22				
CF	1.337			
CCl	1.767			
CH	1.100			
FCF	109.2	−114.2 (−115.3)	12.3 (12.2)	1.47 (1.42)
FCCl	111.1			
FCH	109.4			
ClCH	108.7			
R23				
CF	1.334 (1.332)			
CH	1.099 (1.098)	−172.5 (−166.2)	13.3 (13.9)	1.85 (1.65)
FCF	108.6 (108.8)			
FCH	110.3			
R32				
CF	1.355 (1.357)			
CH	1.099 (1.093)			
FCF	108.3 (108.3)	−106.0 (−108.0)	12.0 (12.7)	2.04 (1.98)
FCH	109.5 (108.7)			
HCH	111.9 (112.5)			
R113				
CF	1.398			
CCl	1.803			
CC	1.579			
FCF	108.0	−171.9 (−185.8)	12.4 (12.0)	0.77

Table 1 (continued)

CFHs	Bond lengths (Å), bond angles (°)	ΔH_{form} (kcal/mol)	I.P. (eV)	μ (D)
FCCl	107.4			
ClCCl	110.2			
FCC	112.2			
ClCC	109.5			
R114				
CF	1.392			
CCl	1.796			
CC	1.548			
FCF	108.8	−213.0 (−219.0)	12.5 (12.2)	0.60 (0.50)
FCCl	108.7			
FCC	110.4			
ClCC	109.3			
R115				
CF	1.393			
CCl	1.795			
CC	1.546			
FCF	109.0	−255.7	12.7 (12.6)	0.64 (0.52)
FCCl	109.0			
FCC	110.3			
ClCC	108.7			
R123				
CF	1.342			
CCl	1.787			
CC	1.521			
CH	1.101			
FCF	107.6	−175.4	12.1	1.72
ClCCl	109.3			
ClCH	106.1			
FCC	110.8			
ClCC	112.9			
HCC	109.1			
R134a				
CF	1.337 (1.335)			
CC	1.509 (1.501)			
CH	1.101 (1.09)			
FCF	108.0	−217.1	12.6	2.05
HCH	107.7			
FCH	107.8			
FCC	111.9			
HCC	110.0			
R142b				
CF	1.340			
CCl	1.771			

Table 1 (continued)

CFHs	Bond lengths (Å), bond angles (°)	ΔH_{form} (kcal/mol)	I.P. (eV)	μ (D)
CC	1.508			
CH	1.101	−115.1	12.2 (12.0)	2.27 (2.14)
FCF	107.6			
HCH	107.3			
FCCl	109.0			
FCC	109.9			
ClCC	111.0			
HCC	111.3			
FCH	109.5 (108.7)			
HCH	111.9 (112.5)			
R143a				
CF	1.339 (1.340)			
CC	1.503 (1.494)			
CH	1.100 (1.081)			
FCF	108.0	−172.6 (−177.9)	13.1 (12.9)	2.33 (2.35)
HCH	107.8			
FCC	110.8			
HCC	111.1 (112)			
R152a				
CF	1.359 (1.364)			
CC	1.506 (1.498)			
CH	1.101 (1.081)			
FCF	107.8	−118.6	11.9 (11.9)	2.27 (2.27)
HCH	108.3			
FCC	110.1 (110.7)			
HCC	110.2 (111.0)			

where R_g is the gas constant. E^* is constructed by multiplying the potential well depth between two non bonded segments of the molecule by the total number of segments per molecule.

According to the procedure proposed in this paper, the three EOS parameters can be estimated as follows: from the values of molecular areas and volumes calculated via the corrected Connolly algorithm and normalized with respect to methane ($r = 1$), the relevant r and σ values can be calculated and, accordingly, V^* and A^* can be obtained by means of Eqs. (4) and (5). The parameter ε/k is obtained from MD as the ratio of the equilibrium value of the nonbonded contributions of the potential energy and the kinetic energy at the given temperature; thus, E^* is easily obtained by Eq. (6).

4. Results and discussion

The validity of any molecular simulation rests on the suitability and accuracy of the equations used for the intermolecular potentials. Although the accuracy of a prediction may be estimated by

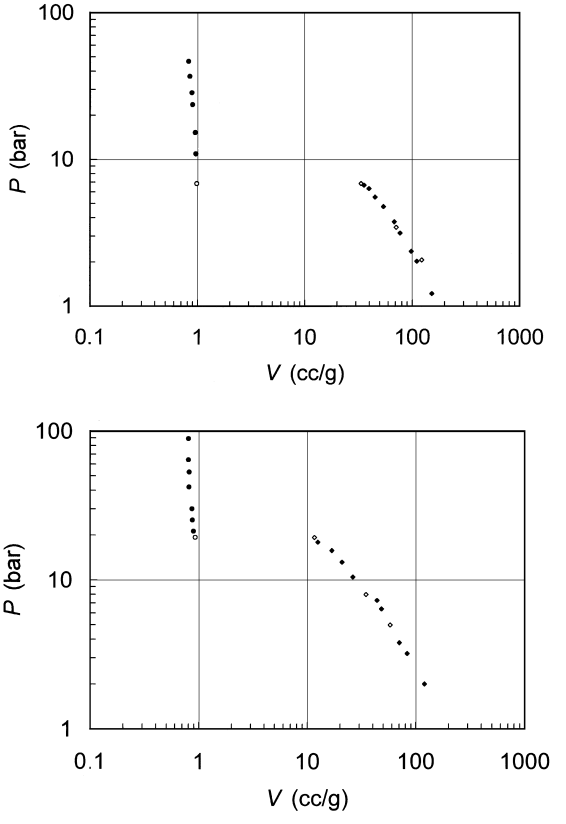

Fig. 3. (a) Simulated PVT behavior of R22 at 323 K. Filled symbols: simulated data. Open symbols: experimental values. (b) Simulated PVT behavior of R142b at 323 K. Filled symbols: simulated data. Open symbols: experimental values.

Table 2
Calculated molecular areas, volumes and PHSCT EOS parameters for all CFHs

CFHs	A (Å^2)	V (Å^3)	A^* (10^{-9} cm^2/mol)	V^* (cm^3/mol)	E^* (bar dm^3/mol)
R13	103 ± 0.2	73.1 ± 0.1	6.16	38.8	32.52
R14	88.5 ± 0.1	73.4 ± 0.1	5.31	31.0	24.37
R21	113 ± 0.2	84.9 ± 0.1	6.78	41.6	52.14
R22	91.1 ± 0.3	58.7 ± 0.2	5.47	36.2	37.42
R23	50.4 ± 0.1	56.1 ± 0.2	5.22	26.8	36.50
R32	69.3 ± 0.1	50.1 ± 0.1	4.16	20.6	34.76
R113	175 ± 0.3	140 ± 0.1	10.5	62.7	70.72
R114	155 ± 0.3	104 ± 0.2	9.26	59.9	53.10
R115	142 ± 0.2	104 ± 0.2	8.50	52.7	44.85
R123	154 ± 0.3	128 ± 0.2	9.27	54.1	64.61
R134a	112 ± 0.1	84.2 ± 0.1	6.76	41.5	45.12
R142b	125 ± 0.2	90.9 ± 0.2	7.47	46.5	49.14
R143a	112 ± 0.2	96.3 ± 0.2	6.73	38.6	43.20
R152a	107 ± 0.3	101 ± 0.1	6.45	35.4	49.29

Table 3
Predicted vapor pressure and volumetric properties for all CFHs
Absolute average deviation (AAD) = $100\times(1)/(N)\Sigma_i|(M^{exp}-M^{calc})/(M^{exp})|$.

CFHs	PVT			VLE			References
	P range (bar)	T range (K)	AAD ρ (%)	P^0 range (bar)	AAD P^0 (%)	AAD V_L (%)	
R13	5–20	150–240	1.79	0.03–15.93	3.36	2.35	[31]
R14	6–20	110–200	1.93	0.07–15.50	1.71	2.27	[31]
R21	3–10	220–310	1.69	0.03–23.96	3.08	3.05	[31]
R22	5–20	250–340	1.59	1.77–19.82	4.62	1.16	[31]
R23	2–10	200–290	1.65	0.03–20.02	5.98	1.78	[31]
R32	12–98	253–333	3.74	3.47–8.64	4.33	2.66	[32]
R113	1–8	270–360	3.09	0.10–15.03	3.12	5.24	[31]
R114	1–8	300–390	1.16	0.11–8.67	4.43	2.91	[31]
R115	1–8	210–300	2.11	0.20–10.88	2.17	2.97	[31]
R123	1.013	203–393	0.622	0.12–21.022	3.30	4.29	[33]
R134a	8–20	285–374	1.79	2.16–4.27	5.34	0.722	[33]
R142b	1.03–3.45	266–350	1.90	1.14–6.20	2.10	1.01	[34]
R143a	5.74–8.26	274–364	2.66	0.25–17.5	2.37	3.76	[35]
R152a	1.03–3.10	266–350	1.01	1.09–14.3	1.42	1.61	[36]

considering the approximations and simplifications of the model and computational procedure, the final test lies in a comparison of theoretically predicted and experimentally measured properties. Table 1 shows the results of this comparison in terms of geometrical parameters and of other general chemico-physical properties (such as dipole moment, ionization potential and enthalpy of formation). From an inspection of this table we can conclude that, for all the CFHs considered, the agreement is more than satisfactory.

We performed a further check of the agreement between simulation and experiment by comparing the simulated PVT behavior of the CFH molecules with the corresponding experimental data. Fig. 3(a) and (b) show, as an example, the results obtained for the two refrigerants R22 and R142b, respectively. Again, the agreement between virtual and real experiment is satisfactory, thus confirming the validity of the particular force field used and the adequacy of the selected simulation conditions.

The next step in our procedure consisted in the calculation of the molecular surfaces A and volumes V of the molecular models reported in Table 1, according to the corrected Connolly algorithm described in the foregoing section. The determination of the relevant values of the PHSCT EOS parameters V^* (Eq. (4)) and A^* (Eq. (5)) is then straightforward. Table 2 reports the values of these parameters for all 14 CFH molecules considered. The last column of Table 2 lists the values of the EOS energetic parameter E^*, obtained by Eq. (6). The corresponding values of the parameter ε/κ, appearing in Eq. (6), were calculated as:

$$\varepsilon/k = \frac{E_{pot}^{nonbonded}}{E_{kin}} T \tag{7}$$

in which the equilibrium energy components were obtained, for all CFHs, from NPT MD simulations in the gas state ($T = 600$ K).

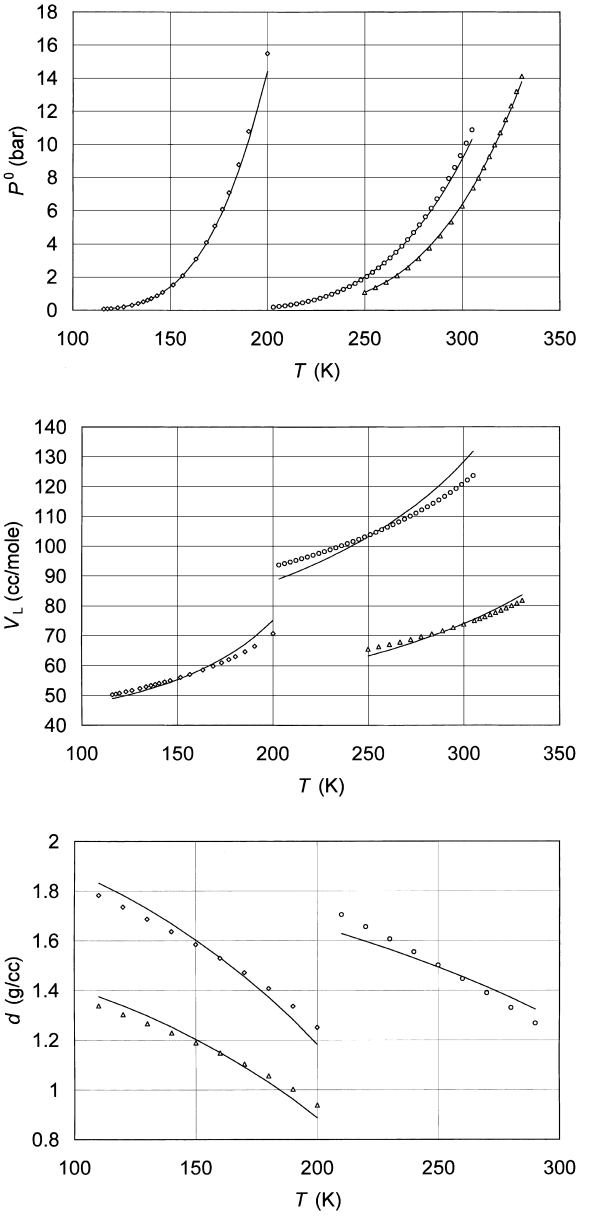

Fig. 4. (a) Simulated vapor pressure as a function of temperature obtained by PHSCT EOS with parameters calculated according to the proposed procedure for a set of CFHs. Symbols: diamonds, R14; circles, R115; triangles, R152a. (b) Simulated saturated liquid volume as a function of temperature obtained by PHSCT EOS with parameters calculated according to the proposed procedure for a set of CFHs. Symbols: diamonds, R14; circles, R115; triangles, R152a. (c) Simulated density as a function of temperature obtained by PHSCT EOS with parameters calculated according to the proposed procedure for a set of CFHs. Symbols: diamonds, R14; circles, R115; triangles, R152a.

In Eq. (7), $E_{\text{pot}}^{\text{nonbonded}}$ is the intermolecular component of the total potential energy; simple order estimation gives that $E_{\text{pot}}^{\text{nonbonded}}$ is proportional to ε and E_{kin} is proportional to kT in the low density and high temperature limit.

Table 4
Comparison in terms of RMSD (see Eq. (8)) between best-fit PHSCT calculations (A) and results from the same EOS with parameter values calculated according to the proposed procedure (B)

CFHs	PVT		VLE			
	Density		Vapor pressure		Saturated liquid density	
	A	B	A	B	A	B
R13	1.97	1.99	2.08	3.69	2.76	2.80
R14	2.22	2.24	2.41	2.37	2.62	2.64
R21	2.12	1.96	2.57	3.42	3.54	3.74
R22	2.48	2.16	1.77	5.36	2.09	1.22
R23	2.04	2.09	2.59	6.71	1.88	2.10
R32	4.63	5.08	0.80	5.11	0.39	4.28
R113	2.77	3.78	2.96	4.14	1.00	6.35
R114	1.42	1.70	1.71	4.94	3.18	3.37
R115	2.55	2.53	2.32	2.54	3.43	3.46
R123	1.65	0.70	2.98	4.13	4.74	4.92
R134a	2.09	2.48	1.35	5.48	0.39	0.81
R142b	2.98	2.06	0.98	2.23	2.03	1.19
R143a	2.74	2.98	2.32	2.37	3.65	3.76
R152a	1.08	1.07	1.39	1.64	1.87	1.83
Average	2.02	**2.34**	2.61	**3.87**	2.34	**3.03**

The a priori calculated parameters reported in Table 2 were inserted in the PHSCT EOS expression and the corresponding thermodynamical properties of the CFHs considered have been predicted. Table 3 gives the predicted vapor pressure and volumetric properties for all CFHs, along with the corresponding average deviations. A graphical example of the comparison between experimental and predicted data is given by Fig. 4(a), (b) and (c), for a selected set of CFHs. In terms of AAD, the quality of the results shown in Table 3 is rather good. Nevertheless, the predicted values show, in all cases, a definite trend in the temperature dependence of the thermophysical properties. A cause for this trend can be reasonably ascribed to the oversimplification of the perturbation term in Eq. (1) that includes, with a certain degree of empiricism, both the van der Waals and the electrostatic interactions. This approximation could be accounted for by including a temperature dependence of the EOS parameters or by explicitly adding a term to the EOS expression. Yet, since the purpose of our paper is to present and test a new procedure for the generation of EOS parameters rather than validating or proposing a new thermodynamic model, we can consider the global prediction results listed in Table 3 more than satisfactory.

It is instructive at this point to consider a comparison of the results obtained by this procedure with the results obtained for the same refrigerants with the same EOS whose optimal values of the parameter were calculated regressing vapor pressure and PVT data [10]. Table 4 shows the results of this comparison in terms of root-mean-square deviation (RMSD), defined as:

$$\mathrm{RMDS} = 100 \sum_i \sqrt{\frac{\left(M_i^{\mathrm{exp}} - M_i^{\mathrm{calc}}\right)^2}{N\left(M_i^{\mathrm{exp}}\right)^2}} \tag{8}$$

where M_i^{exp} is the experimental value of a generic property M, M_i^{calc} is the corresponding calculated value and N is the total number of data points. If we consider that the uncertainty in the experimental data is of the order of 0.2–0.5%, the a priori calculation method proposed in this paper, when compared to pure correlation of experimental data, introduces only approximately 1% of additional uncertainty. If we further take into account the very short times and the low costs required to obtain one set of PHSCT EOS parameters for each CHF molecule (from the molecule building to its MD simulation) and that no one single experimental data is required, even to obtain a prediction of vapor pressure, the quality of the results reported in Table 4 are, in our opinion, to be considered more than satisfactory.

5. Conclusions

This paper reports the results obtained with a new procedure for estimating EOS parameters from computer simulations. The problem of estimating reasonable parameters for EOS is a topical issue in the analysis and synthesis of chemical processes and in the use of process simulators. In this last case, for instance, chemical engineers need to input EOS parameters for molecules that have not yet been synthesized (as it might be the case of a particular chloro-fluoro-hydrocarbon), or for long chain molecules for which experimental data cannot be easily obtained (due to peculiar process or experimental conditions). Furthermore, in the calculation of rate controlled processes, it is sometimes necessary to estimate the equilibrium condition with a high degree of accuracy, and again experimental data in such conditions may not be available.

The new, original method proposed in this work gives good results, is relatively inexpensive, absolutely general and can be applied in principle to any EOS, provided the parameters have a well defined physical meaning. The tuning of the energetic parameter to a generated data accounts for the degree of empiricism introduced at a certain stage in the development of any EOS. Further work is in progress to extend the method to other EOS and to enlarge the data base test substances.

List of symbols

A	molecular surface area
A^*	characteristic molecular surface area, Eq. (5)
a	intermolecular potential well depth between a nonbonded pair of segments, Eqs. (1) and (2)
b	effective hard-sphere diameter, Eqs. (1) and (3)
d	hard-sphere diameter, Eq. (1)
E^*	characteristic cohesive energy, Eq. (6)
E_{kin}	kinetic energy of a system
E_{pot}	potential energy of a system
$E_{pot}^{nonbonded}$	nonbonded contribution of the potential energy of a system
E_{tot}	total energy of a system
$g(d^+)$	pair radial distribution function of hard spheres at contact Eq. (1)
k	Boltzmann constant

N	number of molecules
P	pressure
P^0	vapor pressure
R_g	gas constant
T	absolute temperature
V	molecular volume
V^*	characteristic molecular volume, Eq. (4)
V_L	saturated liquid volume

Greek letters

ε	depth of the minimum in the pair potential, Eqs. (2), (3) and (6)
ρ	number density
σ	pair potential separation distance between segment centers at minimum, Eqs. (2)–(5)

Acknowledgements

The authors wish to thank the Ministero dell'Università e della Ricerca Scientifica (MURST, Roma) and the University of Trieste (special grant for Scientific Research) for the financial support.

Appendix A

The total potential energy E_{pot} of the COMPASS force field is expressed as a combination of valence terms, including diagonal and off-diagonal cross coupling terms, and nonbonded interaction terms. The analytical form of E_{pot} can then be written as:

$$
\begin{aligned}
E_{pot} = {} & \sum_b \left[K_2(b-b_0)^2 + K_3(b-b_0)^3 + K_4(b-b_0)^4 \right] \\
& + \sum_\theta \left[H_2(\theta-\theta_0)^2 + H_3(\theta-\theta_0)^3 + H_4(\theta-\theta_0)^4 + \sum_\phi \left\{ V_1\left[1-\cos\left(\phi-\phi_1^0\right)\right] \right.\right. \\
& \left.\left. + V_2\left[1-\cos\left(2\phi-\phi_2^0\right)\right] + V_3\left[1-\cos\left(3\phi-\phi_3^0\right)\right] \right\} + \sum_\chi K_\chi \chi^2 \sum_b \sum_{b'} F_{bb'}(b-b_0) \right. \\
& \times (b'-b_0') + \sum_\theta \sum_{\theta'} F_{\theta\theta'}(\theta-\theta_0)(\theta'-\theta_0') + \sum_b \sum_\theta F_{b\theta}(b-b_0)(\theta-\theta_0) \\
& + \sum_b \sum_\phi (b-b_0)(V_1\cos\phi + V_2\cos 2\phi + V_3\cos 3\phi) \\
& + \sum_{b'} \sum_\phi (b'-b_0')(V_1\cos\phi + V_2\cos 2\phi + V_3\cos 3\phi) \sum_\theta \sum_\phi (\theta-\theta_0) \\
& \times (V_1\cos\phi + V_2\cos 2\phi + V_3\cos 3\phi) \\
& + \sum_\phi \sum_\theta \sum_{\theta'} K_{\phi\theta\theta'}\cos\phi(\theta-\theta_0)(\theta'-\theta_0') + \sum_{i>j} \frac{q_i q_j}{r_{ij}} + \sum_{i>j} E_{ij}\left[2\left(\frac{r_{ij}^0}{r_{ij}}\right)^9 - 3\left(\frac{r_{ij}^0}{r_{ij}}\right)^6 \right]
\end{aligned}
$$

References

[1] K.E. Gubbins, N. Quirke (Eds.), Molecular Simulations and Industrial Applications, Gordon and Breach, Amsterdam, 1996.
[2] H.J. Bohm, C. Meissner, C.R. Ahlrichs, Mol. Phys. 53 (1984) 651.
[3] C.A. Gough, S.E. DeBolt, P.A. Kollman, J. Comp. Chem. 13 (1992) 963.
[4] S.J. Weiner, P.A. Kollman, D.T. Nguyen, D.A. Case, J. Comp. Chem. 7 (1986) 230.
[5] C. Vega, B. Saager, J. Fischer, J. Mol. Phys. 68 (1989) 1079.
[6] R. Yamamoto, O. Kitao, K. Nakanishi, Fluid Phase Equilibria 104 (1995) 349.
[7] M. Lisal, V. Vacek, Fluid Phase Equilibria 118 (1996) 61.
[8] M. Lisal, V. Vacek, Fluid Phase Equilibria 127 (1997) 83.
[9] M. Fermeglia, A. Bertucco, D. Patrizio, Chem. Eng. Sci. 52 (1997) 1517.
[10] M. Fermeglia, A. Bertucco, S. Bruni, Chem. Eng. Sci. 53 (1998) 3117.
[11] M. Fermeglia, S. Pricl, Fluid Phase Equilibria 158 (1998) 49.
[12] J.R. Maple, U. Dinur, A.T. Hagler, Proc. Natl. Acad. Sci. USA 85 (1988) 5350.
[13] J.R. Maple, M.-J. Hwang, T.P. Stockfisch, U. Dinur, M. Waldman, C.S. Ewig, A.T. Hagler, J. Comput. Chem. 15 (1994) 162.
[14] J.R. Maple, M.-J. Hwang, T.P. Stockfisch, A.T. Hagler, Israel J. Chem. 34 (1994) 195.
[15] M.-J. Hwang, T.P. Stockfisch, A.T. Hagler, J. Am. Chem. Soc. 116 (1994) 2515.
[16] A.K. Rappé, W.A. Goddard, J. Phys. Chem. 95 (1991) 3358.
[17] C.L. Brooks, R. Montgomery, B. Pettitt, M. Karplus, J. Chem. Phys. 83 (1985) 5897.
[18] M. Waldman, M.A.T. Hagler, J. Comput. Chem. 14 (1993) 1077.
[19] M.L. Connolly, J. Appl. Crystallogr. 16 (1983) 548.
[20] M.L. Connolly, Science 221 (1983) 709.
[21] M.L. Connolly, J. Am. Chem. Soc. 107 (1985) 1118.
[22] L.M. Rellick, W.J. Becktel, Biopolymers 42 (1997) 191.
[23] H.J.C. Berendsen, J.P.M. Postma, W.F. van Gunsteren, A. DiNola, J.R. Haak, J. Chem. Phys. 81 (1984) 3684.
[24] H.C. Andersen, J. Chem. Phys. 72 (1980) 2384.
[25] L. Verlet, Phys. Rev. 159 (1967) 98.
[26] Y. Song, E.A. Mason, J. Chem. Phys. 12 (1991) 7840.
[27] Y. Song, S.M. Lambert, J.M. Prausnitz, Ind. Eng. Chem. Res. 33 (1994) 1047.
[28] Y. Song, S.M. Lambert, J.M. Prausnitz, Chem. Eng. Sci. 17 (1994) 2765.
[29] Y. Song, T. Hino, S.M. Lambert, J.M. Prausnitz, Fluid Phase Equilibria 117 (1996) 69.
[30] Y.C. Chiew, Mol. Phys. 70 (1990) 129.
[31] B. Platzer, A. Polt, G. Maurer, Thermophysical Properties of Refrigerants, Springer-Verlag, Berlin, FRG, 1990.
[32] C. Bouchot, D. Richon, Proc. Int. Conf. CFC's: The Day After, Padova (I), 1994, 517.
[33] M.O. McLinden, J.S. Gallagher, L.A. Weber, G. Morrison, D. Ward, A.R.H. Goodwin, M.R. Moldover, J.W. Schmidt, H.B. Chae, T.J. Bruno, J.F. Ely, M.L. Huber, ASHRAE Trans. 95 (1989) 263.
[34] ASHRAE, Thermodynamic Properties of Refrigerants, New York, USA, 1980, 183.
[35] G. Giuliani, S. Kumar, F. Polonara, P. Zazzini, Proc. Int. Conf. CFC's: The Day After, Padova (I), 1994, 525.
[36] ASHRAE, Thermodynamic Properties of Refrigerants, New York, USA, 1980, 189.